Pergamon

SCIENCE DIRECT®

Tetrahedron: *Asymmetry* 14 (2003) 2529–2538

TETRAHEDRON: *ASYMMETRY*

Synthesis and characterization of a new enantiopure hydroxylated phosphine, its rhodium(I) and (III) complexes and their performance in catalytic carbonylation

Josep Duran,[a] Daniel Oliver,[a] Alfonso Polo,[a,*] Julio Real,[b] Jordi Benet-Buchholz[c] and Xavier Fontrodona[c]

[a]*Departament de Química, Universitat de Girona, Campus de Montilivi, 17071 Girona, Spain*
[b]*Departament de Química, Universitat Autònoma de Barcelona, 08193 Bellaterra, Spain*
[c]*Bayer AG, Bayer Industry Services, Analytics X-ray Laboratory, Geb. Q18, Raum 490, D-51368 Leverkusen, Germany*

Received 30 March 2003; accepted 29 May 2003

Abstract—The enantiomerically pure hydroxylated phosphine (1*S*,2*S*,5*R*)-1-diphenylphosphinomethyl-2-isopropyl-5-methyl-cyclohexanol **3** was prepared in a two-step stereoselective process from the commercially available and low cost (−)-menthone. Reaction of this new ligand with the appropriate rhodium precursor gave the respective Rh(I) and Rh(III) complexes. For rhodium(I), the binuclear complex *trans*-P,P-bis-{μ-chlorocarbonyl[(1*S*,2*S*,5*R*)-1-diphenylphosphinomethyl-2-isopropyl-5-methyl-cyclohexanol-*P*]rhodium(I)} **6** was obtained by reaction with $[Rh(\mu\text{-}Cl)(CO)_2]_2$. For Rh(III), two isomeric edge-sharing bioctahedral (ESBO) complexes, *trans*-O,O-*trans*-P,P-bis{(OC-6-32)-μ-chlorodichloro[(1*S*,2*S*,5*R*)-1-diphenylphosphinomethyl-2-isopropyl-5-methyl-cyclohexanol-*O*,*P*]rhodium(III)} **7a** and *trans*-O,O-*cis*-P,P-bis{(OC-6-32)-μ-chlorodichloro[(1*S*,2*S*,5*R*)-1-diphenylphosphinomethyl-2-isopropyl-5-methyl-cyclohexanol-*O*,*P*]rhodium(III)} **7b**, and the partially hydrolyzed product, *trans*-O,O-*cis*-P,P-(OC-6-32)-{μ-chloro-μ-hydroxo-tetrachlorobis[(1*S*,2*S*,5*R*)-1-diphenylphosphinomethyl-2-isopropyl-5-methyl-cyclohexanol-*O*,*P*]-dirhodium(III)}**8** were characterized in solid state by single-crystal X-ray diffraction analysis. The *O*-axial-*P*-equatorial *trans*-*O*,*O* arrangements observed in compounds **7a**,**b** and **8** are preferred over the more common *O*-equatorial-*P*-equatorial structure, presumably due to the stereo-electronic coordination preferences of the chiral hydroxylated phosphine. To the best of our knowledge, the ligand arrangement observed in **7b** and **8** is unique among ESBO complexes. The rhodium(I) complex **6** is active as a catalyst precursor in the hydroformylation of styrene, yielding initial turnover frequencies up to 440 h^{-1} and selectivities up to 74% in the branched aldehyde. Unfortunately, no enantiomeric excesses have been observed within experimental error.

1. Introduction

Although chelating diphosphines are the prevalent chiral bidentate ligands to achieve catalytic asymmetric transformations, the ever increasing need for new catalytic systems has led to the development of mixed-donor ligands such as (P,O), (P,N) and (P,S) donors.[1] Hydroxylated phosphines, a class of hemilabile (P,O)-mixed-donor ligands, have attracted considerable interest in recent years mainly because of their application in homogeneous catalytic reactions,[1–5] with the exception of catalytic carbonylation for which few studies have been described.[6] It is also of interest that the introduction of hydroxyl groups increases the hydrophilicity and allows to obtain water-soluble ligands.[7]

Enantiomerically pure hydroxylated phosphines have been obtained from diastereoselective multi-step synthesis starting from simple aldehydes,[8,9] by resolution of the racemate[10,11] and, more efficiently, by nucleophilic ring-opening of chiral epoxides with phosphides, as this reaction shows high regioselectivity and stereoselectivity.[12,13]

Using the epoxide-opening reaction we have developed a two-step stereoselective synthesis for a new enantiopure hydroxylated phosphine derived from the commercially available, low cost (−)-menthone. Herein we report the synthesis and characterization of this new

* Corresponding author. Fax: +34 (9)72418150; e-mail: alfons.polo@udg.es

0957-4166/$ - see front matter © 2003 Elsevier Ltd. All rights reserved.
doi:10.1016/S0957-4166(03)00488-9

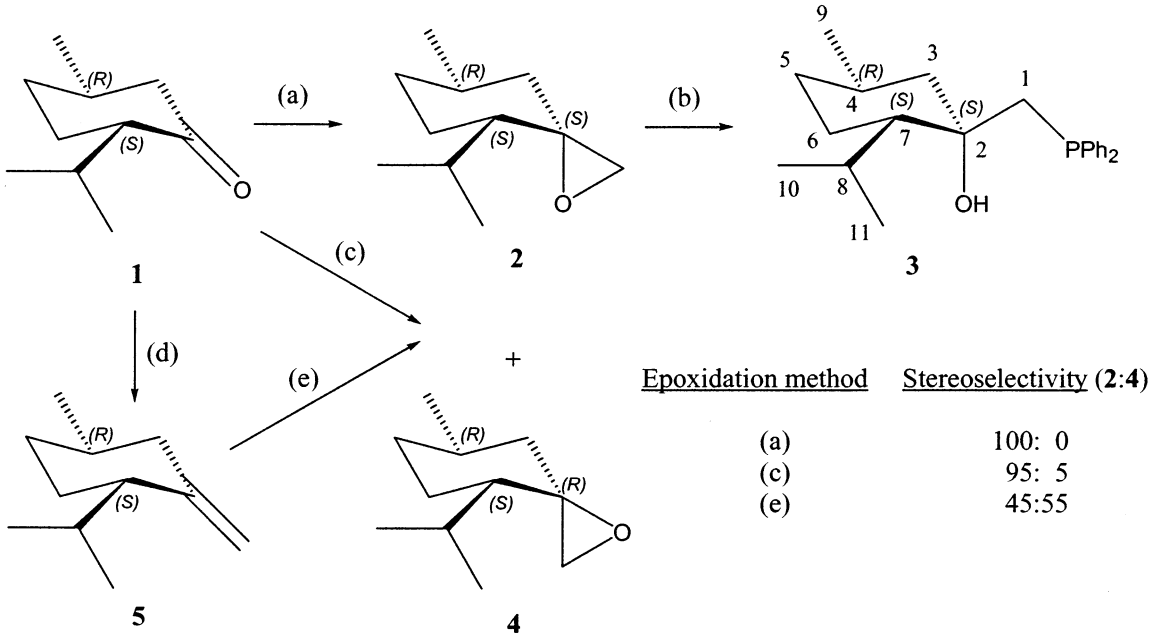

Scheme 1. Synthetic routes for the new enantiopure hydroxylated phosphine **3**. *Reagents and conditions*: (a) $(CH_3)_3SOI/NaH$, DMSO, rt; (b) $KPPh_2$, THF, rt; (c) $CH_3)_3SI/NaH$, DMSO, rt; (d) $(C_6H_5)_3PCH_3Br/NaNH_2$, THF, 0°C; (e) *m*-CPBA/$NaHCO_3$, CH_2Cl_2/H_2O, rt.

enantiomerically pure hydroxylated phosphine, the study of the stereoelectronic effects of this ligand in its rhodium(I) and rhodium(III) coordination complexes, and the performance of the Rh(I) complex as a catalyst precursor in the hydroformylation of styrene.

2. Synthesis of (1*S*,2*S*,5*R*)-1-diphenylphosphinomethyl-2-isopropyl-5-methyl-cyclohexanol, 3

Ligand **3** was prepared from commercially available (−)-menthone **1** in a two-step synthesis according to Scheme 1. In the first step, reaction of **1** with dimethylsulfoxonium methylide, prepared in situ upon treatment of trimethylsulfoxonium iodide with sodium hydride, gave the (1*S*,4*S*,7*R*)-4-isopropyl-7-methyl-1-oxaspiro[2.5]octane **2** in good yield (80%). Epoxide **2** presents the transferred methylene in an equatorial position, according to previously reported results using other cyclohexanones.[14] Treatment of oxirane **2** with 1 equiv. of potassium diphenylphosphide in THF gave the (1*S*,2*S*,5*R*)-1-diphenylphosphinomethyl-2-isopropyl-5-methyl-cyclohexanol **3**, in 76% yield. The attempts to obtain the epoxide isomer **4** via the reaction of (−)-menthone **1** with dimethylsulfonium methylide (Scheme 1), in which the insertion of methylene into the CO double bond is proposed to give preferentially an axial carbon–carbon bond,[14] gave a mixture of the two diastereomeric oxiranes, with oxirane **2** being the major product, surprisingly. It seems that the diastereoselectivity of the reaction is controlled by the configuration of the tertiary carbon near the carbonyl group. Alternatively, an almost equimolecular mixture of oxiranes **2** and **4** was obtained by epoxidation of the olefin **5**, conveniently prepared by a Wittig reaction on (−)-menthone **1**.

Compounds **2**–**5** were characterized by NMR spectroscopy. In compound **3**, the methylenic protons near the phosphine group are diastereotopic, showing a ^2J coupling constant with the phosphorus atom, as it can be seen in the ^1H and $^1H\{^{31}P\}$ NMR spectra (Fig. 1). In the $^{13}C\{^1H\}$ NMR spectrum, the four aliphatic carbons close to the phosphine group (C_1, C_2, C_3, C_7) appear as doublets by coupling to the phosphorus atom. In the $^{31}P\{^1H\}$ NMR spectrum, compound **3** shows a single resonance at −24.87 ppm.

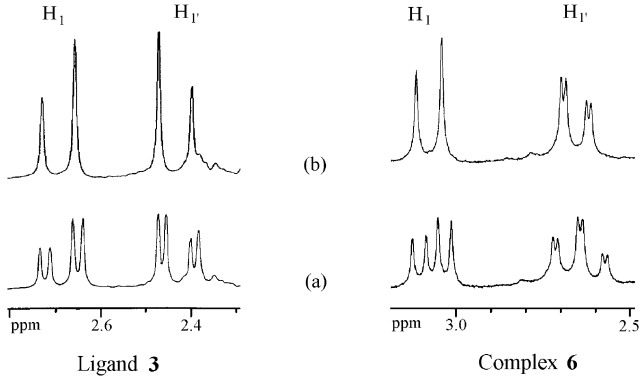

Figure 1. ^1H (a) and $^1H\{^{31}P\}$, (b) NMR spectra of chiral hydroxylated phosphine **3** and its rhodium(I) complex **6**.

3. Coordination of (1*S*,2*S*,5*R*)-1-diphenylphosphinomethyl-2-isopropyl-5-methyl-cyclohexanol 3 to Rh(I)

Addition of 1 equiv. of ligand **3** to a solution of $[Rh(\mu\text{-}Cl)(CO)_2]_2$ at room temperature yields a rhodium complex **6** carrying the enantiopure hydroxylated phosphine. The spectroscopic characteristics of complex **6** are in agreement with a dimeric rhodium(I) structure in which only the phosphine group is coordinated to the metal (Scheme 2). The IR spectrum of complex **6** shows an intense ν(CO) absorption at 1975 cm^{-1}, in agreement with terminal *trans*-coordinated carbonyls (Scheme 2), and a sharp ν(OH) at 3546 cm^{-1} showing that the hydrogen of the hydroxyl group remains in the ligand. In the ^1H NMR spectrum, the methylenic protons near the phosphine group are also diastereotopic (Fig. 1). One of them is a doublet of doublets owing to coupling to both the geminal proton and the phosphorus center. The second resonance consists of a triplet of doublets, arising from two similar coupling constants to the geminal hydrogen and to the phosphorus atom, and a third smaller coupling constant. In the $^{13}C\{^1H\}$ NMR spectrum, three aliphatic carbons (C_1, C_3, C_7) appear as doublets by coupling to the phosphorus atom. In the $^{31}P\{^1H\}$ NMR spectrum, compound **6** shows a doublet by coupling to rhodium ($^1J_{P-Rh}=162.1$ Hz) at 57.95 ppm. This coupling constant is in agreement with a square-planar rhodium(I) complex with a *cis* geometry between the higher *trans*-influence ligand (CO) and the phosphine group.[15]

Attempts to obtain Rh(I) *P*,*O*-chelated complexes with the enantiopure hydroxylated phosphine, by substitution of the chloride ligands by different non-coordinating anions in the presence of PPh_3 or CO have failed. The greater stabilization of the low oxidation state of the metal produced by coordination to the highly π-acceptor ligands, in comparison with the potential stabilization produced by the chelate effect, could be the cause of the observed results.

4. Coordination of (1*S*,2*S*,5*R*)-1-diphenylphosphinomethyl-2-isopropyl-5-methyl-cyclohexanol 3 to Rh(III)

Attempts to obtain X-ray quality crystals of complex **6** by recrystallization in $CHCl_3$/hexane for long periods of time, resulted in the oxidation of the metal, loss of CO and crystallization of the edge-sharing bioctahedral (ESBO) Rh(III) complex $[Rh(\mu\text{-}Cl)Cl_2(\mathbf{3})]_2$ **7** with the *P*,*O*-chelated chiral hydroxylated phosphine. This compound can also be obtained, in a 38% yield, by addition of 1 equiv. of ligand **3** to an ethanol solution of $RhCl_3{\cdot}xH_2O$ at room temperature. In comparison with the Rh(I) complex **6**, the non requirement for π-acceptor ligands to stabilize the higher oxidation state of the metal in **7** promotes the coordination of the hydroxyl group in this case.

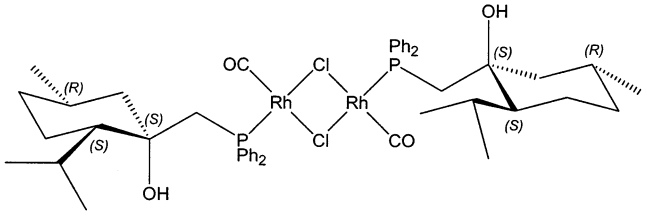

6

Scheme 2. Proposed structure for the chiral hydroxylated phosphine rhodium(I) complex **6**.

Complex **7** is not soluble enough to obtain quality measurements of its $^{13}C\{^1H\}$ NMR. Furthermore, its ^1H NMR spectrum is too complex to extract useful structural information. However, freshly prepared CD_2Cl_2 solutions of the product show, mainly, two resonances, at δ_P 47.68 ($^1J_{P-Rh}=110.8$ Hz) and 38.16 ppm ($^1J_{P-Rh}=123.8$ Hz) in ca. 1:1 intensity ratio, in the $^{31}P\{^1H\}$ spectrum, suggesting the existence in solution of the two isomeric complexes **7a** and **7b** (Scheme 3) that have been characterized in solid state (vide infra). The $^1J_{P-Rh}$ are in agreement with octahedral rhodium(III) complexes with a *O*,*P*-chelated ligand.[15] Although there is not sufficient experimental data to make a definitive assignment of the phosphorus resonances to **7a** and **7b**, the signal with a smaller $^1J_{P-Rh}$ (110.8 Hz, at 47.68 ppm) could be related to isomer **7b**, since the π-donor ability of a bridging chloride in *trans* to both phosphine groups should not be as large as that of a bridging chloride in *trans* to a single phosphine **7a**. Aged CD_2Cl_2 solutions of complex **7** develop a yellow precipitate, with the $^{31}P\{^1H\}$ NMR spectrum showing the disappearance of the signal at 47.68 ppm suggesting that a fractional crystallization has occurred. Unfortunately, these crystals were not of sufficient quality to determine their structure in solid state by XRD methods.

After different crystallizations of complex **7**, crystals of three habits could be distinguished under the microscope. Subsequent crystallographic analysis revealed that they had different unit cell parameters. Three crystals, one of each type, were subjected to XRD crystal structure determination (see Section 6). Selected distances and angles are listed in the captions of Figures 2, 3 and 4. The crystal structure of $\mathbf{7a}{\cdot}\frac{1}{2}H_2O$, although of somewhat low quality (Fig. 2), revealed an ESBO rhodium(III) complex with two chlorides in the bridging positions and the hydroxylated phosphine acting as a chelate ligand with the hydroxyl and phosphine groups in axial and equatorial positions respectively. The *O*-donor groups are mutually in *trans* positions across the dimer, and the same arrangement was observed for the phosphorus atoms resulting in a global structure of type **II** (Scheme 4). The molecule is C_1 symmetry because the inversion center symmetry is broken by the menthane cycles, owing to the stereoelectronic preference of the chelate rings to adopt the δ conformation (vide infra). The crystal structure of $\mathbf{7b}{\cdot}\frac{1}{2}C_6H_{14}$ (Fig. 3) differs from the previous one in the

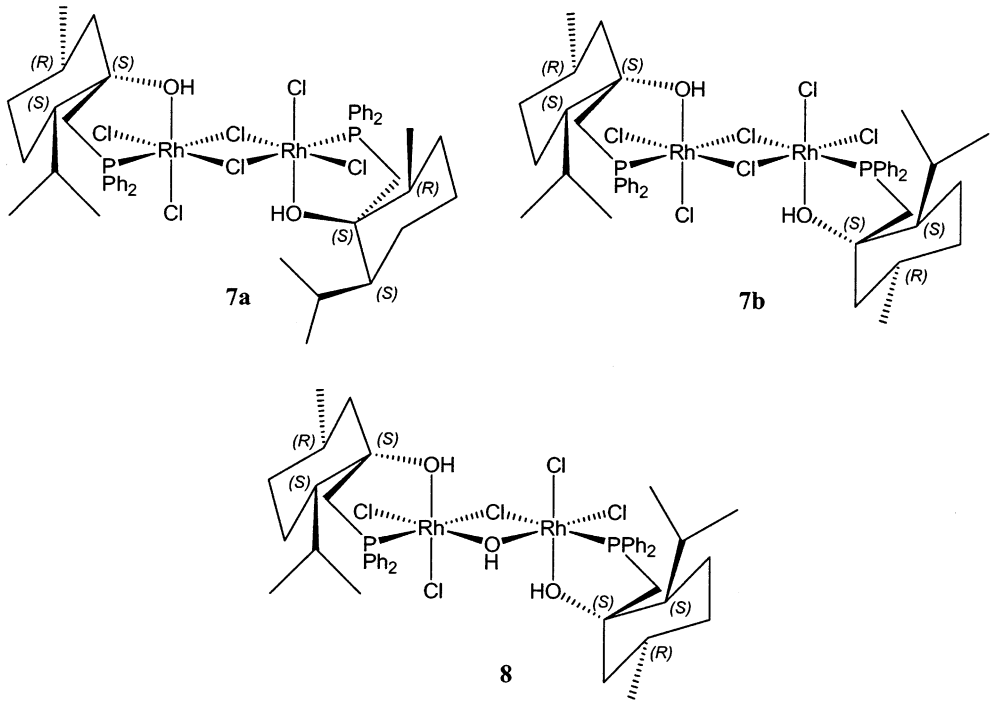

Scheme 3. Structure of the chiral hydroxylated phosphine rhodium(III) complexes (**7a**, **7b** and **8**) characterized in solid state.

relative positions of the phosphine groups, which in this case are in *cis*, adopting a structure of type **V** and pseudo C_2 symmetry (Scheme 4). To the best of our knowledge, this ligand arrangement is unique among comparable edge-sharing bioctahedral complexes. Finally, the crystal structure of **8** (Fig. 3) revealed, as in the case of **7b**, an ESBO rhodium(III) complex with the unusual geometry type **V** but where a bridging chloride has been replaced by a bridging hydroxo ligand. Complex **8** is most likely a product of partial hydrolysis of **7b** in the lengthy crystallization process, but the factors that determine the formation of this product, and not other, are still under study as hydrolysis products may still be relevant in water-containing catalytic processes catalyzed by rhodium complexes (e.g. biphasic catalysis).

In structures **7a**,**b** and **8** the geometry about each rhodium(III) atom is approximately octahedral, however, the planarity of the Rh_2Cl_2 core is slightly distorted in **7a**,**b**, owing most probably to packing forces in the solid state. For complexes **7a**,**b** the Rh–Rh distances (3.553(3) and 3.584(1) Å, respectively) are greater than in the chloro-bridged diphosphine complex $[Rh(\mu\text{-}Cl)Cl_2(dppm)]_2$[16] (3.43 Å), as it could be expected, but shorter than in the monophosphine complex $[Rh(\mu\text{-}Cl)Cl_2(PEt_3)_2]_2$[17] (3.74 Å) with an axial–axial–equatorial–equatorial arrangement of type **VI** (Scheme 4). This suggests that the less hindered *O*-donor ligand allows a greater approach of the two octahedral units, compared to a phosphine group. In complex **8**, with a smaller bridging ligand, the Rh—Rh distance is consequently shorter (3.28 Å). Owing to the chelating effect, the Rh–P distances in **7a**,**b** (2.23 Å) and **8** (2.22 Å) are more similar to those in the chelating phosphinothioether complex $[Rh(\mu\text{-}I)I_2(o\text{-}MeSC_6H_4PPh_2)]_2$[18] (2.27 Å) than to those in the above-mentioned chloro-bridged diphosphine and monophosphine complexes (2.38 and 2.39 Å, respectively).[16,17] Finally, the Rh-Cl(bridging) distances are longer than the Rh-Cl(terminal) distances and are consistent with the *trans* influences of their respective *trans* ligands.

These ESBO rhodium(III) complexes of type $[RhX_3L]_2$ (L = bidentate ligand) are of interest from several different perspectives, including stereoisomerism[19] and stereo and regiospecificity in ligand substitution reactions.[20] In this class of compounds, the bridging positions are always occupied by the X ligands and the distribution of the eight terminal positions can lead, in principle, to numerous stereoisomers. However, the few examples that have been described show structures of type **I**, for the bridging diphosphine $Ph_2PCH_2PPh_2$,[16] and **II**, for the chelating phosphinothioether $o\text{-}MeSC_6H_4PPh_2$.[18] In ESBO complexes of other transition metals (groups IV–VII) with chelating diphosphines the equatorial–equatorial arrangement (type **III**) is normally preferred, rather than axial–equatorial structures (types **II** and **IV**), since close contacts of axial phosphine groups are thus avoided.[21–32] Only for bridging-chelating tetraphosphines[33,34] and for less hindered bidentate ligands, such as dithioethers, axial-equatorial arrangements (type **IV** or **V**, respectively) have been regularly observed.[35,36]

In our case, the hydroxylated phosphine **6** cannot act as a bridging ligand (type **I**), since the observed bite angle (ca. 84°) is incompatible with the Rh–Rh distances, and compounds **7a**,**b** and **8** prefer the *O*-axial-*P*-equatorial

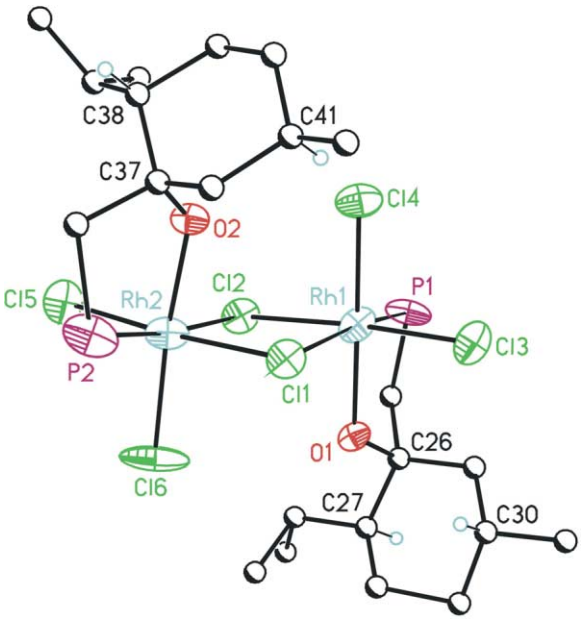

Figure 2. ORTEP plot (50%) of complex **7a**, hydrogen atoms and aryl rings are omitted to fully appreciate the geometry of the complex. Selected distances (Å) and angles (°): P1–Rh1 2.252(8), O1–Rh1 2.13(17), Rh1–Cl4 2.288(7), Rh1–Cl3 2.324(10), Rh1–Cl2 2.356(9), Rh1–Cl1 2.513(8), Cl1–Rh2 2.344(9), Rh2–O2 2.081(17), Rh2–P2 2.206(11), Rh2–Cl5 2.299(11), Rh2–Cl6 2.311(7), Rh2–Cl2 2.455(8), O1–Rh1–P1 83.5(5), O1–Rh1–Cl4 178.6(8), P1–Rh1–Cl4 96.6(3), O1–Rh1–Cl3 91.0(7), P1–Rh1–Cl3 93.4(4), Cl4–Rh1–Cl3 90.4(3), O1–Rh1–Cl2 86.3(7), P1–Rh1–Cl2 91.9(3), Cl4–Rh1–Cl2 92.3(3), Cl3–Rh1–Cl2 173.7(3), O1–Rh1–Cl1 88.6(5), P1–Rh1–Cl1 171.5(3), Cl4–Rh1–Cl1 91.2(3), Cl3–Rh1–Cl1 89.9(3), Cl2–Rh1–Cl1 84.3(3), Rh2–Cl1–Rh1 93.9(2), O2–Rh2–P2 85.4(6), O2–Rh2–Cl5 91.9(7), P2–Rh2–Cl5 87.6(4), O2–Rh2–Cl6 175.5(8), P2–Rh2–Cl6 96.5(4), Cl5–Rh2–Cl6 92.3(4), O2–Rh2–Cl1 85.0(7), P2–Rh2–Cl1 97.1(4), Cl5–Rh2–Cl1 174.1(3), Cl6–Rh2–Cl1 90.6(4), O2–Rh2–Cl2 88.7(6), P2–Rh2–Cl2 173.2(4), Cl5–Rh2–Cl2 89.1(3), Cl6–Rh2–Cl2 89.6(3), Cl1–Rh2–Cl2 85.9(3), Rh1–Cl2–Rh2 95.2(3).

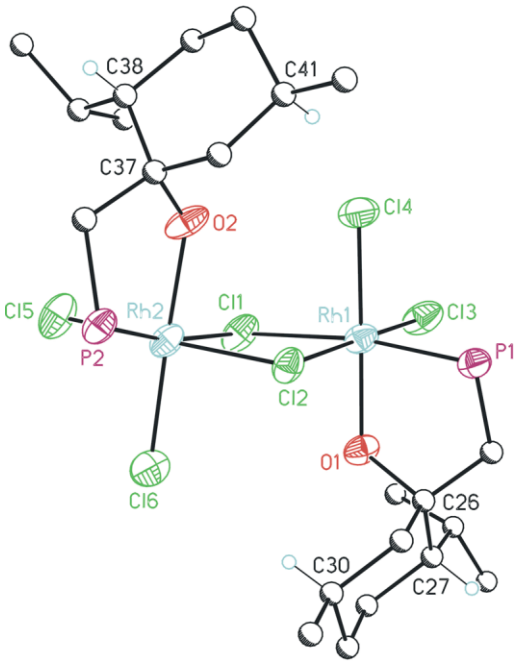

Figure 3. ORTEP plot (50%) of complex **7b**, hydrogen atoms and aryl rings are omitted to fully appreciate the geometry of the complex. Selected distances (Å) and angles (°): Rh1–O1 2.084(5), Rh1–P1 2.239(2), Rh1–Cl4 2.285(2), Rh1–Cl3 2.297(2), Rh1–Cl2 2.357(2), Rh1–Cl1 2.481(2), Cl2–Rh2 2.343(2), Rh2–O2 2.106(5), Rh2–P2 2.230(2), Rh2–Cl6 2.296(2), Rh2–Cl5 2.302(2), Rh2–Cl1 2.475(2), O1–Rh1–P1 84.74(14), O1–Rh1–Cl4 176.98(14), P1–Rh1–Cl4 97.37(8), O1–Rh1–Cl3 88.40(15), P1–Rh1–Cl3 86.88(8), Cl4–Rh1–Cl3 89.56(8), O1–Rh1–Cl2 90.13(15), P1–Rh1–Cl2 94.45(7), Cl4–Rh1–Cl2 91.85(8), Cl3–Rh1–Cl2 177.92(9), O1–Rh1–Cl1 86.98(14), P1–Rh1–Cl1 171.38(8), Cl4–Rh1–Cl1 91.00(8), Cl3–Rh1–Cl1 95.29(8), Cl2–Rh1–Cl1 83.16(7), Rh2–Cl2–Rh1 99.37(7), O2–Rh2–P2 83.19(14), O2–Rh2–Cl6 177.97(16), P2–Rh2–Cl6 98.33(8), O2–Rh2–Cl5 90.34(16), P2–Rh2–Cl5 88.05(8), Cl6–Rh2–Cl5 91.07(8), O2–Rh2–Cl2 89.06(16), P2–Rh2–Cl2 95.15(7), Cl6–Rh2–Cl2 89.45(8), Cl5–Rh2–Cl2 176.65(8), O2–Rh2–Cl1 87.04(14), P2–Rh2–Cl1 170.16(8), Cl6–Rh2–Cl1 91.42(8), Cl5–Rh2–Cl1 93.12(8), Cl2–Rh2–Cl1 83.56(7), Rh2–Cl1–Rh1 92.65(7).

trans-*O*,*O* arrangements (types **II** and **V**) in front of the more sterically unstable *cis*-*O*,*O* geometry (type **IV**). However, differentiation between the preferred arrangements and the *O*-equatorial-*P*-equatorial (type **III**) needs a deeper discussion on the stereochemistry of the chiral ligand.

On account that the preferred conformation for the chiral chelate ring depends on the configuration of the stereogenic carbon, the more voluminous substituent being placed in an equatorial position,[37] the chelate rings of complexes **7a**,**b** and **8** adopt invariably the δ conformation placing both tertiary carbons of the menthane cycle, carrying the isopropyl groups, in equatorial positions. For the observed structures **7a**,**b** and **8** (types **II** and **V**) the preferred conformation of the chelate rings places the menthane cycles in a pseudo-parallel arrangement, but with each one on a different side of the pseudo-planar Rh_2Cl_2 core (Fig. 5). Alternatively, in an hypothetical equatorial–equatorial arrangement (type **III**) the preferred chelate ring conformation would also locate the menthane cycles parallel to each other, but crossing the Rh_2Cl_2 plane (Fig. 5), as we have recently observed for the related ligand, (1*R*,2*S*,5*R*)-1-diphenylphosphinomethyl-2-isopropyl-5-methyl-cyclohexanethiol, in its *trans*-bis(phosphinothiolato)palladium(II) and platinum complexes.[38] Thus, the stereoelectronic preference of the chelate ring to adopt the δ conformation gives rise to an appreciable difference in the structure and stability between complexes with *O*-axial-*P*-equatorial coordination and complexes with *O*-equatorial-*P*-equatorial disposition. The experimental observations seem to indicate that the last situation is energetically disfavored.

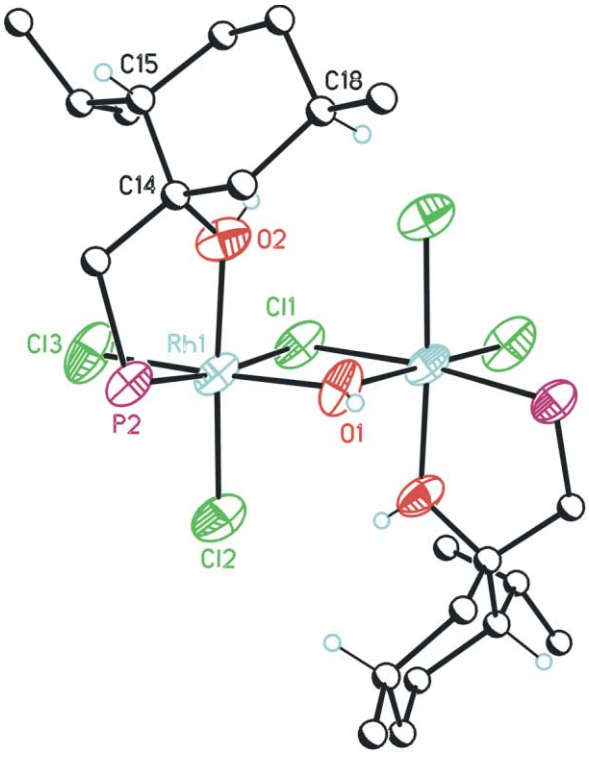

Figure 4. ORTEP plot (50%) of complex **8**, hydrogen atoms and aryl rings are omitted to fully appreciate the geometry of the complex. Selected distances (Å) and angles (°): Rh1–O1 2.062(3), Rh1–O2 2.081(3), Rh1–P2 2.219(2), Rh1–Cl2 2.296(2), Rh1–Cl3 2.317(2), Rh1–Cl1 2.431(2), O1–Rh1–O2 86.93(13), O1–Rh1–P2 97.50(10), O2–Rh1–P2 83.49(12), O1–Rh1–Cl2 90.58(5), O2–Rh1–Cl2 176.66(14), P2–Rh1–Cl2 99.08(7), O1–Rh1–Cl3 175.99(13), O2–Rh1–Cl3 91.36(13), P2–Rh1–Cl3 85.92(7), Cl2–Rh1–Cl3 90.96(7), O1–Rh1–Cl1 84.73(13), O2–Rh1–Cl1 89.54(11), P2–Rh1–Cl1 172.54(5), Cl2–Rh1–Cl1 87.99(5), Cl3–Rh1–Cl1 91.62(6).

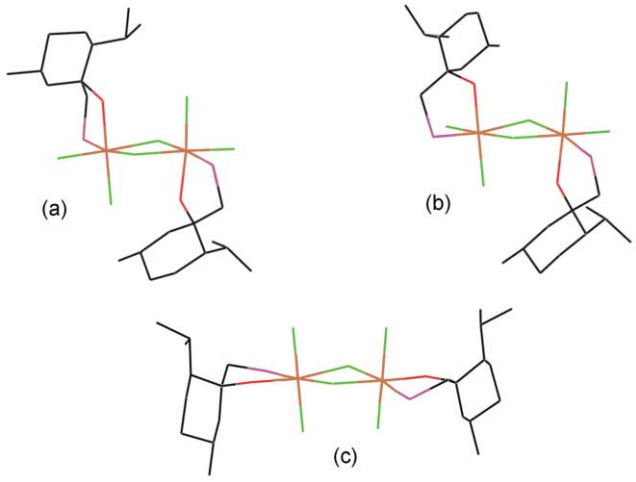

Figure 5. The stereo-electronic preference to place the tertiary carbon of the menthane cycle, carrying the isopropyl group, in equatorial position should produce a dramatic difference in the structure and stability between complexes with *O*-axial-*P*-equatorial coordination (**7a** (a) and **7b** (b)) and complexes with an hypothetical *O*-equatorial-*P*-equatorial coordination of the hydroxylated phosphine (c). Hydrogen atoms and aryl rings are omitted to fully appreciate the geometry of the ligand arrangements.

5. Evaluation of the new chiral hydroxylated phosphine rhodium(I) complexes in the catalytic hydroformylation of styrene

In Table 1 we offer the first data on the evaluation of the hydroxylated phosphine complexes of rhodium(I) as precursors in the catalytic hydroformylation of styrene with carbon monoxide and hydrogen. Catalytic systems formed by the addition of one equivalent of hydroxylated phosphine **3** to the metal precursor $[Rh(\mu\text{-}Cl)(CO)_2]_2$ showed to be highly active in the carbonylation of this vinyl aromatic. Conversions are practically complete after 5–6 h of reaction, except at low temperature (Fig. 6), with initial turn over frequencies up to 440 h^{-1}, although in some cases an activation period (ca. 15 min.) was observed. GC–MS analysis of the final solutions showed that aldehydes were the only

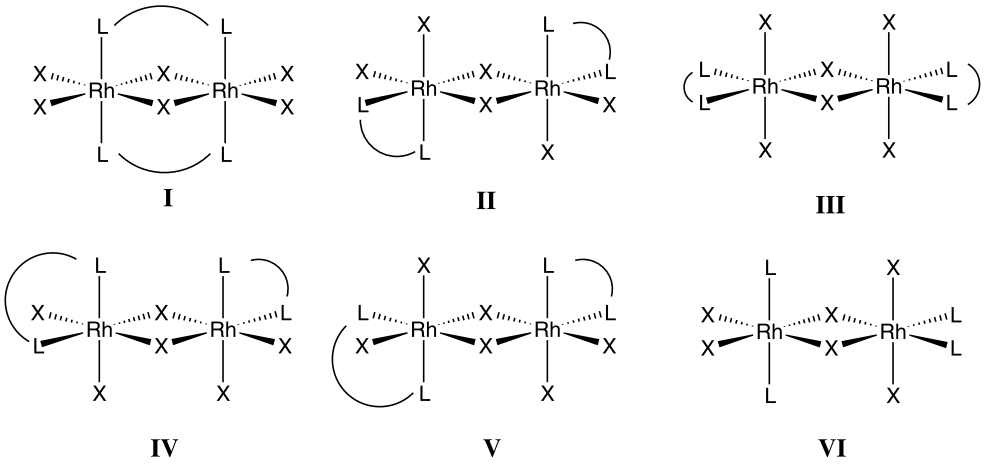

Scheme 4. Structures described for the edge-sharing bioctahedral (ESBO) complexes of transition metals (groups IV–VIII).

Table 1. Hydroxylated phosphine **3** complexes of rhodium(I) as catalyst precursors in the hydroformylation of styrene with CO and H_2 to give 2-phenylpropanal (*iso*) and 3-phenylpropanal (*n*)[a]

3/Rh ratio	Temperature (°C)	Pressure (bar)	H_2/CO ratio	TOF (h^{-1})[b]	*n*/*iso* ratio
1	80	10	1/1	100	49/51
1	80	20	1/1	440	37/63
1	60	20	1/1	120[c]	26/74
2	80	20	1/1	269	36/64
1	80	20	2/1	315[c]	39/61

[a] *Reaction conditions*: styrene, 10.0 mmol; $[Rh_2Cl_2(CO)_4]$, 0.025 mmol; toluene, 27.6 mL; reaction time, 24 h.
[b] Initial turnover frequency measured in the first 30 min of reaction.
[c] Initial turnover frequency measured in the first 30 min after the activation period.

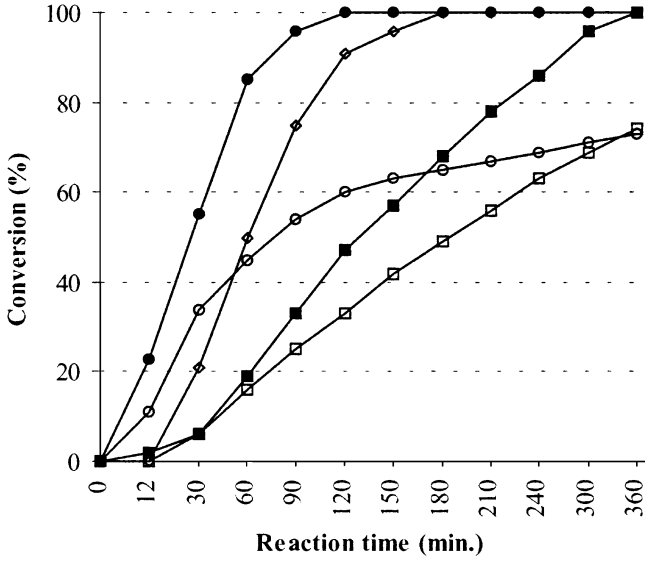

Figure 6. Conversion of styrene into aldehydes versus time. Reaction conditions are indicated in Table 1 (■ entry 1; ● entry 2; □ entry 3; ○ entry 4; ◇ entry 5).

products, only traces of alcohols (<0.5%) were detected. Regarding the regioselectivity, the reaction preferentially produced the branched aldehyde and the selectivity was very sensitive to the reaction temperature and pressure. An increase in the regioselectivity was observed with a decrease in the reaction temperature. Conversely, a decrease in the total pressure produced an equivalent amount of both aldehydes. Other parameters such as the H_2/CO ratio appreciably affected neither the selectivity nor the activity of the reaction. With regard to the enantioselectivity of the reaction, no enantiomeric excess within the experimental error of measurement, were observed, suggesting a monodentate behavior for ligand **3**, at least in the rhodium(I) intermediate species. This is in agreement with the structural data discussed above. However, the increase of the **3**/Rh ratio produces inhibition of the catalytic activity. This observation is surprising since for monodentate ligands, an increase in the activity with the L/Rh ratio is expected, at least up to a L/Rh value of 4.[39] On the other hand, the regio and enantioselectivities do not vary, pointing to a similar catalytic active species that is transformed into inactive complexes in the presence of an excess of the hydroxylated phosphine in the reaction conditions. This ligand effect is not fully understood on the molecular level and is still under study.

6. Experimental

All reactants were commercially obtained and used without further purification. Compounds **2**–**7** were synthesized using standard Schlenk techniques under nitrogen atmosphere. Solvents were dried by standard methods and distilled and deoxygenated before use. Elemental analyses were performed on a Fisons EA-1108 analyzer. Infrared spectra of samples in KBr pellets were recorded on a Mattson Satellite FTIR spectrophotometer. Deuterated solvents for NMR measurements were dried over molecular sieves. Proton NMR spectra were recorded at 200 MHz on a Bruker DPX-200 spectrometer. Peak positions are relative to tetramethylsilane as internal reference. $^{31}P\{^1H\}$ NMR spectra were recorded on the same instrument operating at 81.0 MHz, chemical shifts are relative to external 85% H_3PO_4, with downfield values reported as positive. $^{13}C\{^1H\}$ NMR spectra were recorded on the same instrument operating at 50.3 MHz, chemical shifts are relative to tetramethylsilane as the internal reference. Gas chromatography analyses were performed on a Shimatzu GC-17A in a Tracer TRB-5 capillary column (30 m×0.25 mm diameter) or in a chiral J&W Scientific CYCLODEXB (30 m×0.25 mm diameter), incorporating FID detector. Optical rotations of the products were measured on a krüss P3002 electronic polarimeter equipped with a sodium light source (589 nm). The identification of GC peaks was done by GC–MS analyses on a Thermo Quest Trace GC 2000 in a J&W Scientific DB-5 capillary column (30 m×0.25 mm diameter), incorporating MS detector. Flash chromatography was performed on silica gel 60 A CC. Solvents for chromatography were distilled at atmospheric pressure prior to use. Microdistillation procedures were performed on a Buchi GK-R-51.

6.1. Preparation of (1*S*,2*S*,5*R*)-1-diphenylphosphinomethyl-2-isopropyl-5-methyl-cyclohexanol 3

Step 1. A mixture of NaH (0.92 g, 21.0 mmol, 55%) and $(CH_3)_3SOI$ (4.62 g, 21.0 mmol) in anhydrous DMSO (15 mL), under nitrogen atmosphere, was vigorously stirred at rt for 2 h and placed in an ice bath. A

solution of (−)-menthone (3.84 mL, 20.0 mmol) in anhydrous DMSO (5 mL) was gradually added over 10 min, the reaction mixture was then protected from light and stirred at rt for 24 h. The reaction mixture was poured on ice/water (80 mL) and the aqueous phase extracted with diethyl ether (3×40 mL). The organic phase was washed with water (2×20 mL), dried with magnesium sulphate, filtered, evaporated to dryness, and distilled (70–75°C, 0.1 Torr) to yield liquid (1*S*,4*S*,7*R*)-4-isopropyl-7-methyl-1-oxa-spiro[2.5]octane **2** of purity >97% by GLC (2.69 g, 80%). ^{1}H NMR ($CDCl_3$ sol.): δ 0.80 (d, 3H, H_{10}, $^3J=6.8$ Hz); 0.90 (d, 3H, H_{11}, $^3J=6.8$ Hz); 0.91 (d, 3H, H_9, $^3J=6.5$ Hz); 1.0-1.9 (m, 9H, H_3-H_8); 2.47 (d, 1H, H_1, $^2J=4.5$ Hz); 2.90 (d, 1H, $H_{1'}$, $^2J=4.5$ Hz). ^{13}C{^{1}H} NMR ($CDCl_3$ sol.): δ 18.61 (s, C_9); 21.83 (s, C_{10}); 22.31 (s, CH_{11}); 24.38 (s, C_5); 25.88 (s, C_8); 30.61 (s, C_4); 33.94 (s, C_6); 43.41 (s, C_3); 44.81 (s, C_7); 51.88 (s, C_1); 61.05 (s, C_2).). MS: *m*/*e* 168 (M^+, 5%); 153 (M^+−15, 100%); 125 (M^+−43, 65%); 95 (75%); 81 (85%). $[\alpha]_D^{20}=+7.7$ (*c* 0.015, CH_2Cl_2).

Step 2. (1*S*,4*S*,7*R*)-4-isopropyl-7-methyl-1-oxa-spiro[2.5]octane **2** (200 mg, 1.19 mmol) was slowly added to an ice-cold solution of potassium diphenylphosphide (0.5 M in tetrahydrofuran, 12.7 mL, 6.38 mmol), while stirring under a nitrogen atmosphere. The reaction mixture was then vigorously stirred at rt. After 3 h, deoxygenated methanol (3 mL), deoxygenated saturated ammonium chloride aqueous solution (3 mL), and deoxygenated water (5 mL) were consecutively added to the reaction mixture. The aqueous phase was extracted with diethyl ether (3×15 mL). The organic phase was washed with water (15 mL), dried with magnesium sulphate, filtered and evaporated to dryness. Purification of the crude product by flash chromatography (hexane/ethyl acetate: 9/1) afforded (1*S*,2*S*,5*R*)-1-diphenylphosphinomethyl-2-isopropyl-5-methyl-cyclohexanol **3** as an oil of purity >99% by NMR (334.7 mg, 76%). ^{1}H NMR ($CDCl_3$ sol.): δ 0.7–1.0 (m, 9H, H_9-H_{11}); 1.0-2.0 (m, 8H, H_3-H_6, H_8, OH); 2.17 (m, 1H, H_7); 2.43 (dd, 1H, H_1, $^2J=14.4$ Hz, $^2J_{H-P}=3.4$ Hz); 2.69 (dd, 1H, $H_{1'}$, $^2J=14.4$ Hz, $^2J_{H-P}=4.4$ Hz); 7.2–7.8 (m, 10H, H_{ar}). ^{13}C{^{1}H} NMR ($CDCl_3$ sol.): δ 18.05 (s, C_9); 20.79 (s, C_5); 22.17 (s, C_{10}); 23.35 (s, C_{11}); 25.91 (s, C_8); 28.02 (s, C_4); 34.97 (s, C_6); 41.86 (d, C_1, $^1J_{C-P}=15.5$ Hz); 49.33 (d, C_3, $^3J_{C-P}=12.1$ Hz); 49.52 (d, C_7, $^3J_{C-P}=4.7$ Hz); 75.51 (d, C_2, $^2J_{C-P}=13.7$ Hz); 127–140 (C_{ar}). ^{31}P{^{1}H} NMR ($CDCl_3$ sol.): δ −24.87 (s). MS: *m*/*e* 354 (M^+, 15%); 333 (M^+−18, 5%); 199 (100%); 186 (60%). $[\alpha]_D^{25}=-8.8$ (*c* 0.012, CH_2Cl_2).

6.2. Preparation of mixtures of (1*S*,4*S*,7*R*)-4-isopropyl-7-methyl-1-oxa-spiro[2.5]octane 2 and (1*R*,4*S*,7*R*)-4-isopropyl-7-methyl-1-oxa-spiro[2.5]octane 4

Method A. The procedure described to obtain epoxide **2** from (−)-menthone using $(CH_3)_3SI$ as reactant produced a mixture of oxiranes **2** and **4** (95:5) in an 80% yield.

Method B. **Step 1**. (−)-Menthone (4 mL, 23.15 mmol) was slowly added to an ice-cold solution of a commercial mixture of $NaNH_2$ and $(C_6H_5)_3PCH_3Br$ (14.47 g, 34.2 mmol) in anhydrous THF (15 mL), with stirring under a nitrogen atmosphere. After 3 h, aqueous 25% NaOH (15 mL) was added. The aqueous phase was extracted with diethyl ether (3×10 mL). The organic phase was washed with deoxygenated saturated ammonium chloride aqueous solution until neutrality and deoxygenated water (15 mL), dried with magnesium sulphate, filtered and evaporated to dryness at 35°C. Purification of the crude product by flash chromatography (hexane) afforded liquid (1*S*,4*R*)-1-isopropyl-4-methyl-2-methylene-cyclohexane **5** of purity >99% by GC (3.10 g, 88%). ^{1}H NMR ($CDCl_3$ sol.): δ 0.7–0.9 (m, 9H, H_9-H_{11}); 1.0–1.7 (m, 7H, H_3,H_4-H_7); 1.89 (*ps*oct, 1H, H_8, $^3J\approx6.7$ Hz); 2.28 (dd, 1H, $H_{3'}$, $^2J=11.9$ Hz, $^3J=3.6$ Hz); 4.58 (br.s, 1H, H_1); 4.70 (br.s, 1H, $H_{1'}$). ^{13}C{^{1}H} NMR ($CDCl_3$ sol.): δ 18.98 (s, C_9); 21.38 (s, C_{10}); 22.09 (s, CH_{11}); 27.06 (s, C_8); 27.37 (s, C_5); 33.37 (s, C_6); 33.99 (s, C_4); 44.40 (s, C_3); 49.36 (s, C_7); 106.08 (s, C_1); 151.16 (s, C_2). IR (KBr): δ_{oop} (=CH_2), 890 cm^{-1}; ν(C=CH_2), 1644 cm^{-1}; ν(=CH_2), 3086 cm^{-1}.

Step 2. A solution of *m*-CPBA (4.08 g, 23.7 mmol) in CH_2Cl_2 (25 mL) was added to a mixture containing (1*S*,4*R*)-1-isopropyl-4-methyl-2-methylene-cyclohexane **5** (1.08 g, 7.09 mmol), CH_2Cl_2 (15 mL) and aqueous $NaHCO_3$ (15 mL, 5%). The reaction mixture was protected from light and stirred for 4 h. The aqueous phase was extracted with CH_2Cl_2 (2×10 mL). The organic phase was washed with NaOH 2 M (2×20 mL) and water (15 mL), dried with magnesium sulphate, filtered, evaporated to dryness at 35°C and distilled (70–75°C, 0.1 Torr) to yield a liquid mixture of oxiranes **2** and **4** (1.04 g, 87.5%, 55:45). Data for **4**: ^{1}H NMR ($CDCl_3$ sol.): δ 0.78 (d, 3H, H_{10}, $^3J=6.8$ Hz); 0.91 (d, 3H, H_{11}, $^3J=6.8$ Hz); 0.95 (d, 3H, H_9, $^3J=6.7$ Hz); 0.9–1.9 (m, 9H, H_3-H_8); 2.49 (d, 1H, H_1, $^2J=4.8$ Hz); 2.75 (d, 1H, $H_{1'}$, $^2J=4.8$ Hz). ^{13}C{^{1}H} NMR ($CDCl_3$ sol.): δ 19.53 (s, C_9); 21.67 (s, C_{10}); 22.85 (s, CH_{11}); 24.01 (s, C_8); 24.90 (s, C_5); 31.84 (s, C_6); 32.82 (s, C_4); 42.80 (s, C_3); 46.03 (s, C_7); 51.86 (s, C_1); 60.22 (s, C_2).

6.3. Preparation of *trans*-P,P-bis-{μ-chlorocarbonyl-[(1*S*,2*S*,5*R*)-1-diphenylphosphinomethyl-2-isopropyl-5-methyl-cyclohexanol-*P*]rhodium(I)} 6

Ligand **3** (98 mg, 0.26 mmol) in CH_2Cl_2 (5 mL) was added to a solution of $[Rh_2Cl_2(CO)_4]$ (51 mg, 0.13 mmol) also in CH_2Cl_2 (5 mL). The reaction mixture was stirred at rt for 24 h. The volume was reduced to 3 mL and the product precipitated by the addition of ethyl ether. 68 mg of complex **6** were obtained, 50% yield, as an orange solid. ^{1}H NMR ($CDCl_3$ sol.): δ 0.5–1.1 (m, 9H, H_9-H_{11}); 1.1–2.3 (m, 8H, H_3-H_6, H_8); 2.65 (td, 1H, H_1, $^2J=14.2$ Hz, $^2J_{H-P}=14.2$ Hz, $J=2.6$ Hz); 3.08 (dd, 1H, $H_{1'}$, $^2J=14.2$ Hz, $^2J_{H-P}=8.0$ Hz); 3.67 (br.s, 1H, OH) 7.3–8.2 (m, 10H, H_{ar}). ^{13}C{^{1}H} NMR ($CDCl_3$ sol.): δ 18.77 (s, C_9); 21.54 (s, C_5); 22.25 (s, C_{10}); 23.93 (s, C_{11}); 26.73 (s, C_8); 28.38 (s, C_4); 34.54 (s, C_6); 40.93 (d, C_1, $^1J_{C-P}=25.2$ Hz); 48.57 (d, C_3, $^3J_{C-P}=9.0$ Hz); 49.71 (d, C_7, $^3J_{C-P}=5.2$ Hz); 88.40 (s,

C_2); 127–137 (C_{ar}). $^{31}P\{^1H\}$ NMR ($CDCl_3$ sol.): δ 57.95 (d, $^1J_{Rh-P}=162.1$ Hz). Anal. found: C, 52.57; H, 5.69%. $C_{48}H_{62}Cl_2O_4P_2Rh_2\cdot CH_2Cl_2$ calcd: C, 52.24; H, 5.73%. $[\alpha]_D^{25}=-50.9$ (c 0.011, CH_2Cl_2).

6.4. Preparation of bis{(OC-6-32)-μ-chlorodichloro-[(1*S*,2*S*,5*R*)-1-diphenylphosphinomethyl-2-isopropyl-5-methyl-cyclohexanol-*O*,*P*]rhodium(III)} 7

Ligand **3** (111 mg, 0.30 mmol) in ethanol (5 mL) was added to a solution of $RhCl_3\cdot xH_2O$ (77.2 mg, 0.30 mmol) also in ethanol (15 mL). The reaction mixture was stirred at rt. After 24 h the volume was reduced to 10 mL and the orange precipitate that appeared, was filtered and washed with cold ethanol (2 mL). The recovered solid shows a low carbon and hydrogen analysis suggesting that some unreacted $RhCl_3$ was also precipitated with the desired product. By successive solid–liquid extractions with CH_2Cl_2 and evaporation of the solvent, a solid (64 mg, 38%) with satisfactory elemental analysis (vide infra) were obtained. $^{31}P\{^1H\}$ NMR (CD_2Cl_2 sol.): δ 47.68 ($^1J_{P-Rh}=110.8$ Hz); 38.16 ($^1J_{P-Rh}=123.8$ Hz). Anal. found: C, 48.23; H, 5.70%. $C_{46}H_{62}Cl_6O_2P_2Rh_2\cdot\frac{1}{2}H_2O$ calcd: C, 48.61; H, 5.59%.

6.5. X-Ray structure determinations

Compound **7a** crystallizes from CH_2Cl_2 giving non homogeneous crystals of poor quality. Only after several attempts, a small crystal could be measured leading to the structure described. No better data set of **7a** could be obtained. Suitable crystals of **7b** were grown by slow evaporation of a chloroform/*n*-hexane mixture 1:1 at 60°C. Crystals of **8** were obtained by slow evaporation of chloroform at rt. All three compounds lead to soft crystals which are difficult to handle and decompose upon manipulation. All measured crystals diffracted giving broad reflections with somewhat low resolution.

Measurements were made on a Siemens P4 diffractometer equipped with a SMART-CCD-1000 area detector, MoKα radiation from a MACScience Co rotating anode source, a graphite monochromator and a Siemens low temperature device LT2 (T = −120°C). The measurements were made in the range 1.65–30.07°. Full sphere data was collected, ω and φ scans. Programs used: Data collection, Smart 5.625 (Bruker-AXS 2001); data reduction, Saint Plus Version 1.6 (Bruker-Nonius 2002); absorption correction, SADABS V. 2.03 (2002) and structure solution and refinement, SHELXTL Version 6.12 (Sheldrick, 2000).

Compound **7a**: $C_{46}H_{60}Cl_6O_{2.5}P_2Rh_2$, $M_r=1133.40$; monoclinic; space group $P2_1$, $a=11.685(2)$ Å, $b=16.840(3)$ Å, $c=13.192(2)$ Å, $\beta=103.294(5)°$, $V=2526.2(8)$ Å^3, $Z=2$, $\rho_{calcd}=1.490$ Mg/m^3, $\mu=1.070$ mm^{-1}, 19161 reflections were collected of which 8512 were unique ($R_{int}=0.173$), 3545 $F_o>4\sigma(F_o)$, 490 refined parameters, $R_1=0.095$, $wR_2=0.2177$, Goodness of fit on $F^2=1.036$, Flack parameter 0.05(15), maximum residual electron density 1.565 (−1.604) e Å^{-3}.

Compound **7b**: $C_{52}H_{74}NCl_6O_2P_2Rh_2$, $M_r=1211.57$; orthorhombic; space group $P2_12_12_1$, $a=13.3659(7)$ Å, $b=16.5154(8)$ Å, $c=26.0653(13)$ Å, $V=5753.7(5)$ Å^3, $Z=4$, $\rho_{calcd}=1.399$ Mg/m^3, $\mu=0.944$ mm^{-1}, 61730 reflections were collected of which 12515 are unique ($R_{int}=0.170$), 6329 $F_o>4\sigma(F_o)$, 490 refined parameters, $R_1=0.0559$, $wR_2=0.1015$, Goodness of fit on $F^2=0.858$, Flack parameter −0.03(4), maximum residual electron density 0.569 (−0.575) e Å^{-3}.

Compound **8**: $C_{23}H_{31.50}Cl_{12.50}O_{1.50}P_1Rh_1$, $M_r=(554.49)\times2$; tetragonal; space group $P4_12_12$, $a=14.0399(11)$ Å, $c=26.401(3)$ Å, $V=5204.2(8)$ Å^3, $Z=8$, $\rho_{calcd}=1.415$ Mg/m^3, $\mu=0.988$ mm^{-1}, 55517 reflections were collected of which 5133 are unique ($R_{int}=0.18$), 3789 $F_o>4\sigma(F_o)$, 266 refined parameters, $R_1=0.0481$, $wR_2=0.0952$, Goodness of fit on $F^2=1.038$, Flack parameter 0.01(5), maximum residual electron density 0.399 (−0.649) e Å^{-3}.

Crystallographic data (excluding structure factors) for the structures in this paper have been deposited with the Cambridge Crystallographic Data Centre as supplementary publication numbers CCDC 206965, CCDC 206964 and CCDC 206963. Copies of the data can be obtained, free of charge, on application to CCDC, 12 Union Road, Cambridge, CB2 1EZ, UK [fax: +44(0)-1223-336033 or e-mail: deposit@ccdc.cam.ac.uk].

6.6. Hydroformylation experiments

A toluene (27.6 mL) solution of styrene (10 mmol), previously stirred with alumina for 24 h at −24°C, $[Rh(\mu\text{-}Cl)(CO)_2]_2$ (0.025 mmol) and the corresponding amount of the hydroxylated phosphine, prepared under nitrogen atmosphere was introduced into an evacuated reactor *Chemipress* (Trallero & Schlee S. L.) and heated with stirring. Once the system reached thermal equilibrium, the gas mixture was introduced to reach the working pressure. During the reaction, the pressure was maintained at a constant by introducing a gas mixture from a gas ballast. The drop of pressure in the ballast was monitored using a pressure transducer connected to an electronic measurement and printing unit. After each run, the reactor was cooled, its contents removed and analyzed by GC–MS. In order to measure the enantiomeric excess of the reaction, a sample of the freshly obtained reaction mixture (2 mL) was slowly added to a suspension of $LiAlH_4$ (50 mg) in anhydrous THF (5 mL). After 15 min, methanol (2 mL) and aqueous HCl (0.5 M, 10 mL) were consecutively added. The aqueous phase was extracted with dichloromethane (3×10 mL) and the organic phase was dried with magnesium sulphate and analyzed by GC in a J&W Scientific CYCLODEXB (30 m×0.25 mm diameter) column.

Acknowledgements

This work was financially supported by the DGESIC, projects PB98-0913-C02 and BQU2002-04070-C02-01.

References

1. Agbossou-Niedercorn, F. In *Applied Homogeneous Catalysis with Organometallic Compounds*; Comils, R.; Herrmann, W. A., Eds.; VCH, 2002; Vol. 2, pp. 1014–1033.
2. Börner, A. *Eur. J. Inorg. Chem.* **2001**, 327–337.
3. Swamamura, M.; Ito, Y. *Chem. Rev.* **1992**, *92*, 857–871.
4. Lahuerta, P.; Moreno, E.; Monge, A.; Muller, G.; Pérez-Prieto, J.; Sanaú, M.; Stiriba, S. E. *Eur. J. Inorg. Chem.* **2000**, 2481–2485.
5. Borns, S.; Kadyrov, R.; Heller, D.; Baumann, W.; Spannenberg, A.; Kempe, R.; Holz, J.; Börner, A. *Eur. J. Inorg. Chem.* **1998**, 1291–1295.
6. Frohning, C. D.; Kohlpaintner, C. W.; Bohnen, H.-W. In *Applied Homogeneous Catalysis with Organometallic Compounds*; Comils, R.; Herrmann, W. A., Eds.; VCH, 2002; Vol. 1, pp. 85–89.
7. Brauer, D. J.; Machnitzki, P.; Nickel, T.; Stelzer, O. *Eur. J. Inorg. Chem.* **2000**, 65–73.
8. Enders, D.; Berg, T. *Synlett* **1996**, 796–798.
9. Enders, D.; Berg, T.; Raabe, G.; Runsink, J. *Liebigs Ann./Recueil* **1997**, 345–363.
10. Albert, J.; Cadena, J. M.; Granell, J. *Tetrahedron: Asymmetry* **1997**, *8*, 991–994.
11. López, C.; Bosque, R.; Sainz, D.; Solans, X.; Font-Bardía, M. *Organometallics* **1997**, *16*, 3261–3266.
12. Muller, G.; Sainz, D. *J. Organomet. Chem.* **1995**, *495*, 103–111.
13. Brunner, H.; Sicheneder, A. *Angew. Chem., Int. Ed. Engl.* **1988**, *27*, 718.
14. Corey, E. J.; Chaykovsky, M. *J. Am. Chem. Soc.* **1965**, *87*, 1353–1364.
15. Parish, R. V. *NMR, NQR, EPR, and Mössbauer Spectroscopy in Inorganic Chemistry*; Ellis Horwood, 1990; pp. 61–69.
16. Cotton, F. A.; Dunbar, K. R.; Eagle, C. T.; Falvello, L. R.; Price, A. C. *Inorg. Chem.* **1989**, *28*, 1754–1757.
17. Cotton, F. A.; Kang, S.-J.; Mandal, S. K. *Inorg. Chim. Acta* **1993**, *206*, 29–39.
18. Dilworth, J. R.; Morales, D.; Zheng, Y. *J. Chem. Soc., Dalton Trans.* **2000**, 3007–3015.
19. Poli, R.; Torralba, R. C. *Inorg. Chim. Acta* **1993**, *212*, 123–134.
20. Cotton, F. A.; Eglin, J. L.; Kang, S.-J. *J. Am. Chem. Soc.* **1992**, *114*, 4015–4016.
21. Cotton, F. A.; Falvello, L. R.; Najjar, R. C. *Inorg. Chem.* **1983**, *22*, 375–377.
22. Cotton, F. A.; Roth, W. J. *Inorg. Chem.* **1983**, *22*, 3654–3656.
23. Cotton, F. A.; Diebold, M. P.; O'Connor, C. J.; Powell, G. L. *J. Am. Chem. Soc.* **1985**, *107*, 7438–7445.
24. Agaskar, P. A.; Cotton, F. A.; Dunbar, K. R.; Falvello, L. R.; O'Connor, C. J. *Inorg. Chem.* **1987**, *26*, 4051–4057.
25. Cotton, F. A.; Eglin, J. L.; James, C. A.; Luck, R. L. *Inorg. Chem.* **1992**, *31*, 5308–5315.
26. Cotton, F. A.; Murillo, C. A.; Petrukhina, M. A. *J. Organomet. Chem.* **1999**, *573*, 78–86.
27. Canich, J. A. M.; Cotton, F. A. *Inorg. Chem.* **1987**, *26*, 4236–4240.
28. Cotton, F. A.; Diebold, M. P.; Roth, W. J. *Inorg. Chem.* **1987**, *26*, 4130–4133.
29. Poli, R.; Owens, B. E. *Gazz. Chim. Ital.* **1991**, *121*, 413–417.
30. Cotton, F. A.; Diebold, M. P.; Kibala, P. A. *Inorg. Chem.* **1988**, *27*, 799–804.
31. Morse, P. M.; Wilson, S. R.; Girolami, G. S. *Inorg. Chem.* **1990**, *29*, 3200–3202.
32. Hermes, A. R.; Girolami, G. S. *Inorg. Chem.* **1990**, *29*, 313–317.
33. Cotton, F. A.; Englin, J. L.; James, C. A. *Inorg. Chem.* **1993**, *32*, 687–694.
34. Cotton, F. A.; Hong, B.; Shang, M.; Stanley, G. G. *Inorg. Chem.* **1993**, *32*, 3620–3627.
35. Cotton, F. A.; Fanwick, P. E.; Fitch, J. W. *Inorg. Chem.* **1978**, *17*, 3254–3257.
36. Heyen, B. J.; Powell, G. L. *Inorg. Chem.* **1990**, *29*, 4574–4576.
37. Brugat, N.; Duran, J.; Polo, A.; Real, J.; Álvarez-Larena, A.; Piniella, J. F. *Tetrahedron: Asymmetry* **2002**, *13*, 569–577.
38. Duran, J.; Brugat, N.; Polo, A.; Real, J.; Fontrodona, X.; Benet-Buchholz, J. *Organometallics*, submitted, CCDC 201836 and CCDC 213436.
39. See Ref. 6, pp. 45–60.